Synthesis of Mixed-Valence Platinum Triangulo Clusters $[Pt_3(\mu\text{-}PPh_2)_2(\mu\text{-}C_6F_5)(C_6F_5)(PPh_2R)_2]$ (R = Ph, Me, Et). Crystal Structures of $[Pt_3(\mu\text{-}PPh_2)_2(\mu\text{-}C_6F_5)(C_6F_5)(PPh_3)_2]$ and $[Pt_3(\mu\text{-}AgOClO_3)(\mu\text{-}PPh_2)_2(\mu\text{-}C_6F_5)(C_6F_5)(PPh_3)_2]$†

Larry R. Falvello, Juan Forniés,* Consuelo Fortuño, Fernando Durán, and Antonio Martín

Departamento de Química Inorgánica and Instituto de Ciencia de Materiales de Aragón, Universidad de Zaragoza-CSIC, 50009 Zaragoza, Spain

Received January 16, 2002

The reaction between $[(C_6F_5)_2Pt(\mu\text{-}PPh_2)_2Pt(PPh_2R)_2]$ and $[Pt(C_7H_{10})_3]$ in toluene yields the triangulo complexes $[Pt_3(\mu\text{-}PPh_2)_2(\mu\text{-}C_6F_5)(C_6F_5)(PPh_2R)_2]$ (R = Ph **4**, Me **5**, Et **6**), which contain two phosphido and one pentafluophenyl bridging ligands and two phosphines and one pentafluophenyl terminal ones. The triangulo metal core displays three Pt−Pt bonds, as expected for a 42 valence electron count cluster. The basicity of these metal cores is demonstrated through the reaction of one of the complexes (R = Ph) with $AgClO_4$ or $[Ag(OClO_3)(PPh_3)]$, which gives the corresponding adduct $[Pt_3(AgOClO_3)(\mu\text{-}PPh_2)_2(\mu\text{-}C_6F_5)(C_6F_5)(PPh_3)_2]$ (**7**) or $[Pt_3Ag(\mu\text{-}PPh_2)_2(\mu\text{-}C_6F_5)(C_6F_5)(PPh_3)_3][ClO_4]$ (**8**). The X-ray structures of **4** and **7** have been determined.

Introduction

The interest in the chemistry of metal clusters with bridging μ-PR_2 groups arises in part from the electronic properties and the geometrical flexibility of these ligands.[1] Such flexibility allows easy closing up of the metal centers, to form metal−metal bonds, depending on the total valence electron count.

In the course of our current research on the synthesis of polynuclear complexes we have studied the reactivity of several palladium or platinum phosphido derivatives toward other metal complexes in order to prepare complexes of higher nuclearity. A judicious choice of the starting materials allows the rational synthesis of binuclear,[2] trinuclear,[2d,3] and tetranuclear[2a,4] derivatives which, depending on the total valence electron count, display metal−metal bonds.

As far as the trinuclear derivatives are concerned, we have prepared symmetric[3c] (**A**) and asymmetric[3a] (**B**) homo- or heterotrinuclear derivatives (Scheme 1) with 48 valence electron counts and in which the metal centers are supported only by the bridging ligands. A two-electron oxidation of the symmetric anion $[(C_6F_5)_2Pt(\mu\text{-}PPh_2)_2Pt(\mu\text{-}PPh_2)_2Pt(C_6F_5)_2]^{2-}$ yields the trinuclear 46 valence electron count cluster in which two platinum centers are not only bridged by the phosphido ligands but linked by a metal−metal bond as well (Scheme 1, **C**). The reaction of the binuclear $[(C_6F_5)_2Pt(\mu\text{-}PPh_2)_2Pt(C_6F_5)_2]^{2-}$ with $[Pt(C_6F_5)_2(thf)_2]$, which acts in this case as a pentafluorophenyl scavenger, results in the formation of the trinuclear complex $[Pt_3(\mu\text{-}PPh_2)_2(C_6F_5)_5]^-$ (Scheme 1, **D**), which, by virtue of the special coordination of one of the phosphido ligands [μ_3-PPh(1,2-η^2-Ph)-κ^3P], has a 44 valence electron count, two Pt−Pt bonds being necessary to satisfy the electron requirements of the metal centers and the metal environments being very different from each other.[3b] The structure of this Pt(II) complex, which contains a bent trinuclear metal skeleton (see Scheme 1), is rather different from the open triangular metal skeleton present in the palladium and/or platinum clusters $[Pd_3(\mu\text{-}Cl)(\mu\text{-}PPh_2)_2(PR_3)_3]^+$,[5] $[Pd_3(\mu\text{-}PBu^t_2)_3Cl(CO)_2]$,[6] $[Pd_3(\mu\text{-}PCy_2)_2(\mu\text{-}SPh)(PCy_2H)_2(SPh)]$,[7] $[Pt_3(\mu\text{-}PPh_2)_3Ph(PPh_3)_2]$,[8] $[Pt_3(\mu\text{-}PBu^t_2)_3H(CO)_2]$,[9] and $[Pd_2Pt(\mu\text{-}Cl)(\mu\text{-}PPh_2)_2(PPh_3)_3]^+$,[5] in which the metal centers display fractional metal oxidation states lower

† Polynuclear Homo- or Heterometallic Palladium(II)-Platinum(II) Pentafluorophenyl Complexes Containing Bridging Diphenylphosphido Ligands. 11. For part 10 see ref 3c.

(1) (a) Garrou, P. E. *Chem. Rev.* **1985**, *85*, 171. (b) Sappa, E.; Tiripicchio, A.; Braunstein, P. *Coord. Chem. Rev.* **1985**, *65*, 219. (c) Sappa, E.; Tiripicchio, A.; Carty, A. J.; Toogood, G. E. *Prog. Inorg. Chem.* **1987** *35*, 437. (d) Ginsburg, R. E.; Rothrock, R. K.; Finke, R. G.; Collman, J. P.; Dahl, L. F. *J. Am. Chem. Soc.* **1979**, *101*, 6550. (e) Rosenberg, S.; Geoffroy, G. L.; Rheingold, A. L. *Organometallics* **1985**, *4*, 1184. (f) Brauer, D. J.; Hessler, G.; Knuppel, P. C.; Stelzer, O. *Inorg. Chem.* **1990**, *29*, 2370.

(2) (a) Forniés, J.; Fortuño, C.; Navarro, R.; Martínez, F.; Welch, A. J. *J. Organomet. Chem.* **1990**, *394*, 643. (b) Falvello, L. R.; Forniés, J.; Fortuño, C.; Martínez, F. *Inorg. Chem.* **1994**, *33*, 6242. (c) Alonso, E.; Casas, J. M.; Cotton, F. A.; Feng, X.; Forniés, J.; Fortuño, C.; Tomás, M. *Inorg. Chem.* **1999**, *38*, 5034. (d) Alonso, E.; Forniés, J.; Fortuño, C.; Martín, A.; Orpen, A. G. *Organometallics* **2001**, *20*, 850.

(3) (a) Alonso, E.; Forniés. J.; Fortuño, C.; Tomás, M. *J. Chem. Soc., Dalton Trans.* **1995**, 3777. (b) Alonso, E.; Forniés, J.; Fortuño, C.; Martín, A.; Orpen, A. G. *J. Chem. Soc., Chem. Commun.* **1996**, 231. (c) Alonso, E.; Casas, J. M.; Forniés, J.; Fortuño, C.; Martín, A.; Orpen, A. G.; Tsipis, C. A.; Tsipis, A. C. *Organometallics* **2001**, *20*, 5571.

(4) (a) Alonso, E.; Forniés, J.; Fortuño, C.; Martín, A.; Rosair, G. M.; Welch, A. J. *Inorg. Chem.* **1997**, *36*, 4426. (b) Falvello, L. R.; Forniés, J.; Fortuño, C.; Martín, A.; Martínez-Sariñena, A. P. *Organometallics* **1997**, *16*, 5849. (c) Alonso, E.; Forniés, J.; Fortuño, C.; Martín, A.; Orpen, A. G. *Organometallics* **2000**, *19*, 2690.

(5) Berry, D. E.; Bushnell, G. W.; Dixon, K. R.; Moroney, P. M.; Wan, C. *Inorg. Chem.* **1985**, *24*, 2625.

(6) Arif, A. M.; Heaton, D. E.; Jones, R. A.; Nunn, C. M. *Inorg. Chem.* **1987**, *26*, 4228.

(7) Sommovigo, M.; Pasquali, M.; Marchetti, F.; Leoni, P.; Beringhelli, T. *Inorg. Chem.* **1994**, *33*, 2651.

(8) Taylor, N. J.; Chieh, P. C.; Carty, A. J. *J. Chem. Soc., Chem. Commun.* **1975**, 448.

(9) Leoni, P.; Manetti, S.; Pasquali, M.; Albinati, A. *Inorg. Chem.* **1996**, *35*, 6045.

10.1021/om020036v CCC: $22.00
Publication on Web 04/30/2002

Scheme 1

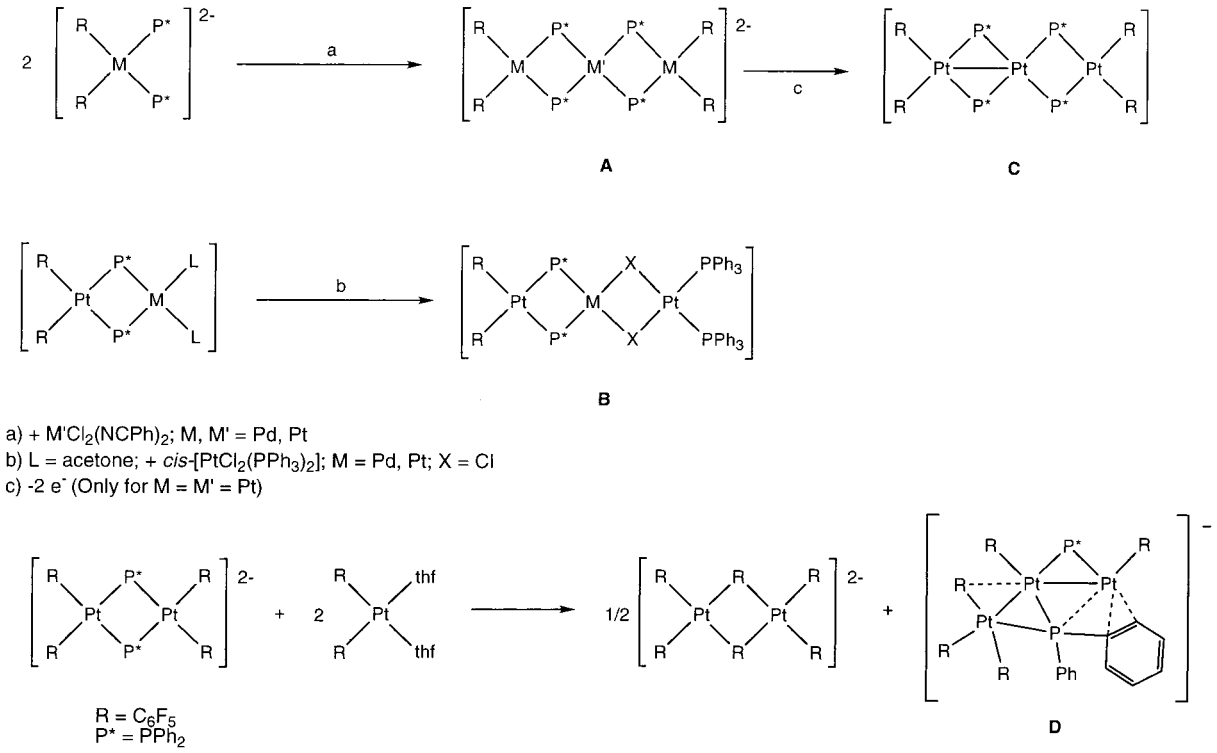

than II and the coordination environments of the metal centers are rather similar to each other (three terminal and three bridging ligands). One of the complexes, $[Pt_3(\mu\text{-}PPh_2)_3Ph(PPh_3)_2]$, is a good example of reversible skeletal isomerism,[10] one of the isomers containing, as expected, two Pt−Pt bonds, while the other contains three, albeit weaker, Pt···Pt interactions. The total valence electron counts in these clusters allow one to infer the number of M−M bonds present in them. Nevertheless, we note that recently Leoni et al. have reported the triangulo phosphido cluster $[Pd_3(\mu\text{-}PBu_3)_2(CN{-}C_6H_4\text{-}p\text{-}Me)_5](CF_3SO_3)_2$, which, despite its 44-electron count, seems to display three Pd−Pd bonds.[11]

In this paper, we report a method for the synthesis of $[Pt_3(\mu\text{-}PPh_2)_2(\mu\text{-}C_6F_5)(C_6F_5)(PPh_2R)_2]$, a 42 valence electron count triangulo derivative, via a condensation process involving the dinuclear diphenylphosphido platinum(II) derivatives $[(C_6F_5)_2Pt(\mu\text{-}PPh_2)_2Pt(PPh_2R)_2]$ and the mononuclear platinum(0) compound $[Pt(C_7H_{10})_3]$. We have also studied their behavior as Lewis bases.

Triangulo phosphido complexes with 42 valence electron counts should display three metal−metal bonds, and although rather scarce,[12,13] there are some fully characterized Pt_3 complexes, namely, $[Pt_3(\mu\text{-}PPh_2)_2(\mu\text{-}H)(PPh_3)_3]^+$ [12a] and $[Pt_3(\mu\text{-}Ph)(\mu\text{-}PPh_2)(\mu\text{-}SO_2)Ph(PPh_3)_2]$.[13] In general, the formation of these phosphido M_3 clusters with two (44 e^-) or three metal−metal bonds (42 e^-) has been attained in the past through unpredictable procedures, and a rational synthetic pathway to these derivatives has not been found until now.

(10) (a) Bender, R.; Braunstein, P.; Dedieu, A.; Ellis, P. D.; Huggins, B.; Harvey, P. H.; Sappa, E.; Tiripicchio, A. *Inorg. Chem.* **1996**, *35*, 1223. (b) Bender, R.; Braunstein, P.; Tiripicchio, A.; Tiripicchio Camellini, M. *Angew. Chem., Int. Ed. Engl.* **1985**, *24*, 861.

(11) Leoni, P.; Vichi, E.; Lencioni, S.; Pasquali, M.; Chiarentin, E.; Albinati, A. *Organometallics* **2000**, *19*, 3062.

(12) (a) Bellon, P. L.; Cerioti, A.; Demartin, F.; Longoni, G.; Heaton, B. *J. Chem. Soc., Dalton Trans.* **1982**, 1671. (b) Fortunelli, A.; Leoni, P.; Marchetti, L.; Pasquali, M.; Sbrana, F.; Selmi, M. *Inorg. Chem.* **2001**, *40*, 3055.

(13) Evans, D. G.; Hughes, G. R.; Mingos, D. M. P.; Bassett, J.-M.; Welch, A. J. *J. Chem. Soc., Chem. Commun.* **1980**, 1255.

Results and Discussion

Synthesis of $[(C_6F_5)_2Pt(\mu\text{-}PPh_2)_2Pt(PPh_2R)_2]$ (R = Ph 1, Me 2, Et 3). Complexes **1**−**3**, which were used as starting materials for the preparation of the triangular platinum clusters, have been prepared by reacting the tetranuclear derivative $[NBu_4]_2[(C_6F_5)_2Pt(\mu\text{-}PPh_2)_2Pt(\mu\text{-}Cl)_2Pt(\mu\text{-}PPh_2)_2Pt(C_6F_5)_2]$ with an excess of the phosphine PPh_2R (R = Ph, Me, Et) in CH_2Cl_2/MeOH according to Scheme 2, a. These asymmetric dinuclear complexes with a total valence electron count of 32 are crystallized from the respective solutions as yellow solids.

The $^{31}P\{^1H\}$ NMR spectra of **1**−**3** show two well-separated sets of signals due to the two types of P atoms (PPh_2R and PPh_2 groups). The resonances due to the bridging PPh_2 groups appear at very high field: −97.5 (**1**), −104.3 (**2**), and −109.3 ppm (**3**), indicating the absence of metal−metal bonds in the complexes (see later), as can be expected for these dinuclear 32-electron complexes. In each complex, the spectrum shows a pattern consistent with an AA′XX′ spin system for the four P atoms. Not all of the signals in the two parts of the spectrum can be identified, and only the value of N ($J_{AX} + J_{AX'}$) can be extracted. Both signals show platinum satellites (^{195}Pt, I = 1/2, 33.7% abundance) from which $^1J_{Pt-P}$ values can be obtained (see Experimental Section).

Complexes **1**−**3**, which contain two equivalent C_6F_5 groups, should display ^{19}F NMR spectra corresponding to an AA′MXX′ system. Complex **1** shows three signals due to *o*-F, *m*-F, and *p*-F atoms in a 4:4:2 intensity ratio. For complexes **2** and **3** the signals due to *m*- and *p*-F

Scheme 2

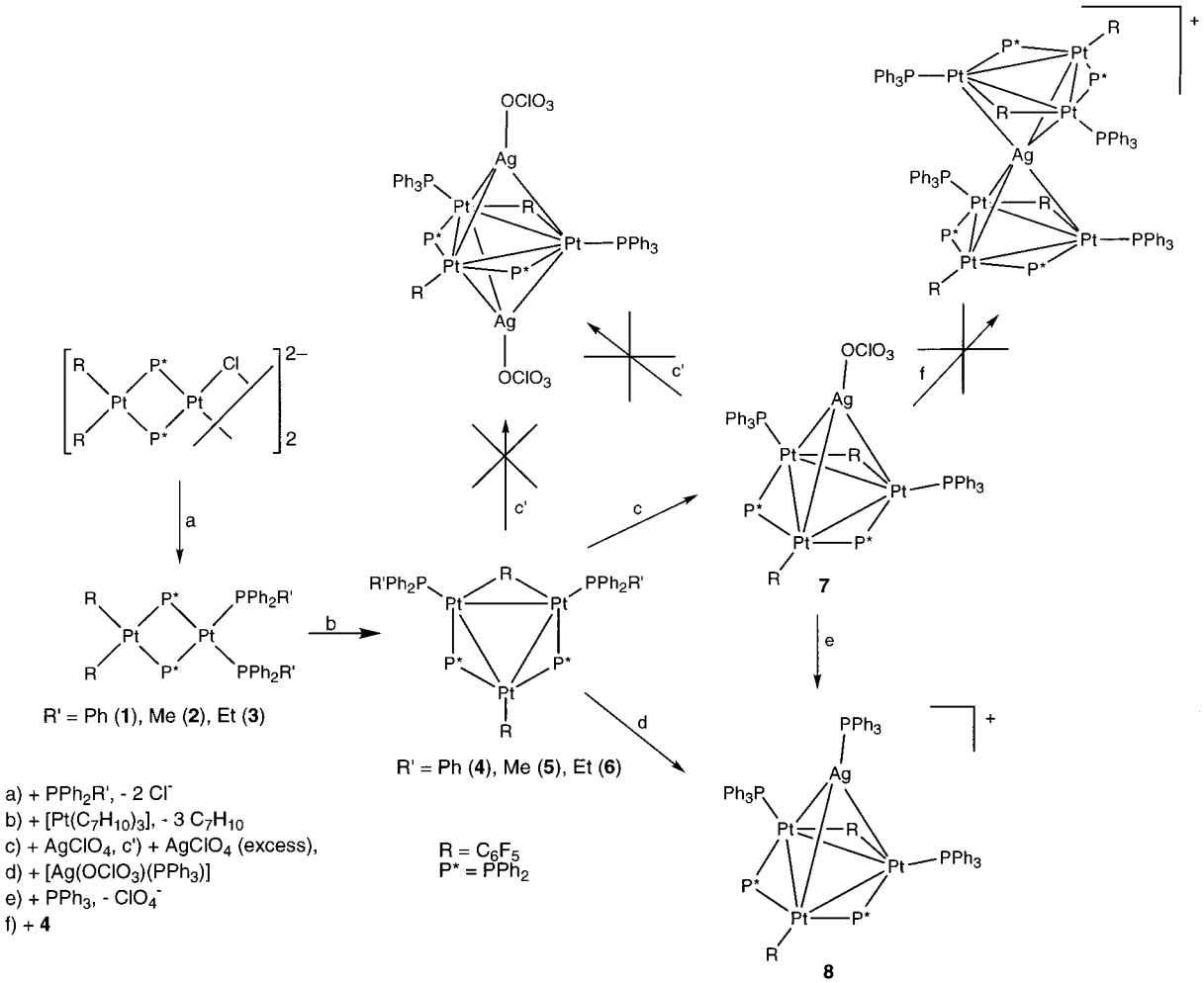

atoms are overlapped (see Experimental Section) and the relative intensities of the *o*- and *m*- + *p*-signals (4:6) are in accord with the proposed structure.

The IR spectra of complexes **1**−**3** show the characteristic absorptions of the pentafluorophenyl group[14] near 1500, 1050, 950, and 800 cm^{-1}. The bands due to the X-sensitive mode of the C_6F_5 groups (ca. 800 cm^{-1}) appear in all cases as two absorptions of similar intensities, as expected for complexes containing two C_6F_5 groups bonded to the same metal in *cis* positions.

Synthesis of $[Pt_3(\mu\text{-}PPh_2)_2(\mu\text{-}C_6F_5)(C_6F_5)(PPh_2R)_2]$ (R = Ph 4, Me 5, Et 6). By reacting equimolecular amounts of the dinuclear diphenylphosphido Pt(II) derivatives **1**−**3** and the mononuclear Pt(0) complex $[Pt(C_7H_{10})_3]$ in toluene at room temperature, dark purple solutions are obtained, and after workup purple crystalline solids are isolated (Scheme 2, b). These solids are identified by elemental analysis, IR and NMR spectroscopy, and a single-crystal X-ray diffraction study carried out on complex **4**, as the neutral Pt_3 triangulo clusters $[Pt_3(\mu\text{-}PPh_2)_2(\mu\text{-}C_6F_5)(C_6F_5)(PPh_2R)_2]$ (R = Ph **4**, Me **5**, Et **6**), with the platinum atoms in a formal oxidation state of 1.33.

Crystal Structure of $[Pt_3(\mu\text{-}PPh_2)_2(\mu\text{-}C_6F_5)(C_6F_5)(PPh_3)_2]$. The structure of complex **4** together with the atom labeling scheme is shown in Figure 1. Selected

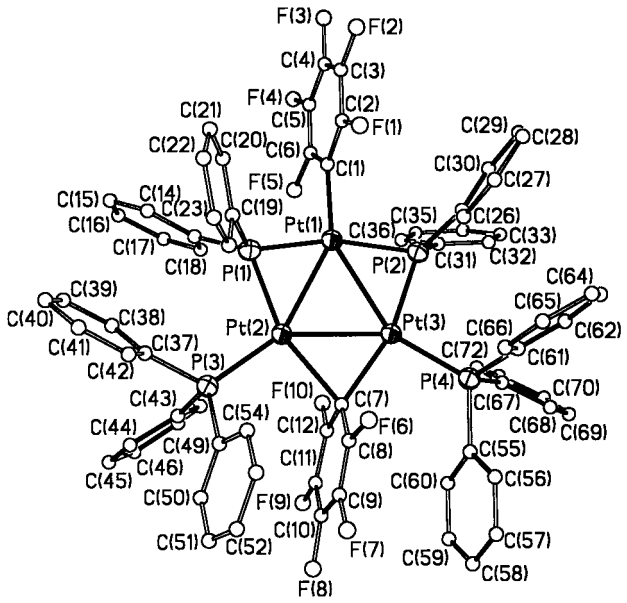

Figure 1. Structure of $[Pt_3(\mu\text{-}PPh_2)_2(\mu\text{-}C_6F_5)(C_6F_5)(PPh_3)_2]$ (**4**).

bond distances and angles are listed in Table 1. The three platinum atoms lie at the corners of an equilateral triangle. The Pt−Pt distances are all very similar and indicative of the existence of intermetallic bonds (Pt(1)−Pt(2) 2.791(1) Å, Pt(1)−Pt(3) 2.791(1) Å, Pt(2)−

(14) Usón, R.; Forniés, J. *J. Adv. Organomet. Chem.* **1988**, *28*, 188.

Table 1. Selected Bond Lengths (Å) and Angles (deg) for $[Pt_3(\mu\text{-}PPh_2)_2(\mu\text{-}C_6F_5)(C_6F_5)(PPh_3)_2]$ (4)

Pt(1)−Pt(2)	2.791(1)	Pt(1)−Pt(3)	2.791(1)	Pt(2)−Pt(3)	2.818(1)
Pt(1)−C(1)	2.046(8)	Pt(1)−P(1)	2.233(2)	Pt(1)−P(2)	2.256(2)
Pt(2)−P(1)	2.219(2)	Pt(2)−P(3)	2.265(2)	Pt(2)−C(7)	2.320(9)
Pt(3)−C(7)	2.165(8)	Pt(3)−P(2)	2.253(2)	Pt(3)−P(4)	2.254(2)
P(1)−C(13)	1.805(9)	P(1)−C(19)	1.822(10)	P(2)−C(25)	1.815(10)
P(2)−C(31)	1.820(9)				

C(1)−Pt(1)−P(1)	99.7(3)	C(1)−Pt(1)−P(2)	97.6(3)
P(1)−Pt(1)−P(2)	161.26(8)	Pt(2)−Pt(1)−Pt(3)	60.64(2)
P(1)−Pt(2)−P(3)	103.01(8)	P(1)−Pt(2)−C(7)	158.8(2)
P(3)−Pt(2)−C(7)	97.9(2)	Pt(1)−Pt(2)−Pt(3)	59.68(2)
C(7)−Pt(3)−P(2)	162.0(2)	C(7)−Pt(3)−P(4)	95.5(2)
P(2)−Pt(3)−P(4)	101.00(8)	Pt(1)−Pt(3)−Pt(2)	59.68(2)
Pt(2)−P(1)−Pt(1)	77.64(8)	Pt(3)−P(2)−Pt(1)	76.49(7)

Pt(3) 2.818(1) Å). Each edge of the triangle is supported by a bridging ligand (two diphenylphosphides and a pentafluorophenyl group). The coordination environment of each metal atom is completed by a terminal ligand (two triphenylphosphine ligands and a pentafluorophenyl group). The four phosphorus atoms and the *ipso* C atom of the terminal C_6F_5 group are roughly coplanar with the platinum centers. The bridging pentafluorophenyl group is not bisected by the molecular plane, but deviates out of the plane in such a way that the *ipso* C(7) atom is 0.41 Å away from the best least-squares plane defined by the Pt and P atoms, while C(10) and F(8) are 1.09 and 1.41, Å respectively, out of the same plane. Both pentafluorophenyl rings are planar and are nearly perpendicular to the plane defined by the Pt and P atoms, the dihedral angles being 81.3° for the terminal group and 85.7° for the bridging one.

The Pt−P and Pt(1)−C(1) distances are in the ranges usually found for these bonds.[2−4] The Pt−P−Pt angles are small, in keeping with the fact that the phosphido ligands are supporting metal−metal bonds.

The presence of a bridging pentafluorophenyl group is noteworthy. Although complexes containing bridging phenyl groups are not rare,[15] there are very few examples in which the C_6F_5 group acts as an electron-deficient bridging ligand. Most of the cases described so far involve dinuclear platinum complexes in which two pentafluorophenyl groups simultaneously bridge the two metal centers, $[Pt_2(\mu\text{-}C_6F_5)_2(C_6F_5)_4]^{2-}$,[16] $[Pt_2(\mu\text{-}C_6F_5)_2(C_6F_5)_4]^{-}$,[17] $[(C_6F_5)_4(\mu\text{-}C_6F_5)_2Pt_2Ag(L)]^{-}$ (L = OEt_2, SC_4H_8).[18] In two cases, there is only one bridging C_6F_5 group and another bridging ligand: $[Pt_2(\mu\text{-}C_6F_5)(\mu\text{-}C_6F_5\text{-}Cl)(C_6F_5)_4]^{-}$ [17] and $[Pt_2(\mu\text{-}C_6F_5)(\mu\text{-}H)(C_6F_5)_2(PPh_3)_2]$.[19] Finally, we have reported an example, the trinuclear cluster $[Pt_3(\mu\text{-}C_6F_5)(C_6F_5)_4(\mu\text{-}PPh_2)_2]^{-}$,[3b] in which there is a very asymmetrical bridging C_6F_5 ligand, the Pt−C_{ipso} distances being 2.108(10) and 2.621(10) Å (see Scheme 1, **D**). In **4**, the bridging pentafluorophenyl group is located asymmetricaly, with rather different Pt−C_{ipso} distances: Pt(2)−C(7) 2.320(9) Å and Pt(3)−C(7) 2.165(8) Å. The ring is slightly tilted toward Pt(2), as occurs to a much greater extent with the more asymmetrical bridge in the previously mentioned complex $[Pt_3(\mu\text{-}C_6F_5)(C_6F_5)_4(\mu\text{-}PPh_2)_2]^{-}$.

Table 2. $^{31}P\{^1H\}$ NMR Data for Complexes 4−8 in $CDCl_3$ (δ in ppm, J in Hz)

	4	5	6	7	8[a]
$\delta_{1,2}$	172.8	168.5	171.7	161.5	161.8
$\delta_{3,4}$	36.8	20.7	34.0	31.6[b]	30.9[c]
J_{12}	313	320	316	317	310
J_{34}	79	82	77	66	59
J_{15}	2356	2386	2350	1920	1913
J_{16}	2640	2569	2666	2312	2293
J_{17}	−102	−107	−107	−78	−101
J_{35}	133	121	130	33	34
J_{36}	3890	3715	3739	4291	4226
J_{37}	312	274	287	167	183

[a] P atom of $AgPPh_3$ fragment: 13.9 ppm. [b]Doublet, 31 Hz (see text). [c]Doublet, 29 Hz (see text).

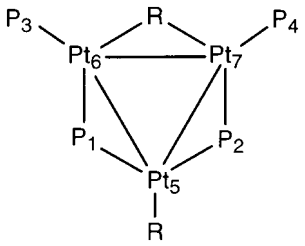

Figure 2. Numbering scheme used in the discussion of the NMR spectra of complexes **4**−**8**.

The $^{31}P\{^1H\}$ NMR spectra of **4**−**6** are similar, and they are in accord with the solid-state structure determined for complex **4**. All data obtained from the spectra are collected in Table 2. The spectra show only one signal at low field: 172.8, 168.5, and 171.7 ppm for **4**, **5**, and **6**, respectively, due to the P atoms of the PPh_2 groups (P1 and P2, see Figure 2 for atom numbering) and one signal (36.8, 20.7, and 34.0 ppm, respectively) due to the P atoms of the PPh_2R groups (P3 and P4). In each region, the central line, due to the isotopomer that does not contain ^{195}Pt (isotopomer A 29% abundance) is a sharp singlet. Coupling between the P atoms of the PPh_2 groups and those of the PPh_2R groups was not observed.

Each singlet signal is flanked by platinum satellites due to the isotopomers in which one of the Pt atoms is ^{195}Pt ($^{195}Pt(5)$, isotopomer B, 14.8% abundance; ^{195}Pt-(6) or $^{195}Pt(7)$, isotopomer C, 29.6% abundance), in which two Pt atoms are ^{195}Pt ($^{195}Pt(5)$ and $^{195}Pt(6)$ or $^{195}Pt(7)$, isotopomer D, 15.1% abundance; $^{195}Pt(6)$ and $^{195}Pt(7)$, isotopomer E, 7.6% abundance), and in which all three metal centers are ^{195}Pt (isotopomer F, 3.9% abundance).

The subspectrum due to isotopomer B can be analyzed as a first-order spin system and consists of a doublet ($^1J_{Pt5-P1,2}$) centered at $\delta_{P1,P2}$ and a doublet ($^2J_{Pt5-P3,4}$) centered at $\delta_{P3,P4}$. In isotopomer C P1 and P2 are inequivalent as are P3 and P4. The subspectrum consists of 8 lines (AA′X spin system) which symmetrically flank the central singlet due to P1 and P2 and from which $^2J_{P1-P2}$, $^1J_{Pt6-P1}$, and $^2J_{Pt7-P1}$ values can be obtained, and 8 lines (two doublets of doublets) which

(15) (a) Dickson, R. S.; Fallon, G. D.; Zhang, Q.-Q. *J. Chem. Soc., Dalton Trans.* **2000**, 1973. (b) Xiaoming He; Ruhlandt-Senge, K.; Power, P. P. *J. Am. Chem. Soc.* **1994**, *116*, 6963. (c) Cabeza, J. A.; Franco, R. J.; Llamazares, A.; Riera, V.; Pérez-Carreño, E.; Van der Maelen, J. F. *Organometallics* **1994**, *13*, 55. (d) Heintz, R. A.; Ostander, R. L.; Rheingold, A. L.; Theopold, K. H. *J. Am. Chem. Soc.* **1994**, *116*, 11387. (e) Solari, E.; Musso, F.; Gallo, E.; Floriani, C.; Re, N.; Chiesi-Villa, A.; Rizzoli, C. *Organometallics* **1995**, *14*, 552265.

(16) Usón, R.; Forniés, J.; Tomás, M.; Casas, J. M.; Navarro, R. *J. Chem. Soc., Dalton Trans.* **1989**, 169.

(17) Usón, R.; Forniés, J.; Tomás, M.; Casas, J. M.; Cotton, F. A.; Falvello, L. R.; Feng, X. *J. Am. Chem. Soc.* **1993**, *115*, 4145.

(18) (a) Usón, R.; Forniés, J.; Tomás, M.; Casas, J. M.; Cotton, F. A.; Falvello, L. R.; Llusar, R. *Organometallics* **1988**, *7*, 2279. (b) Casas, J. M.; Forniés, J.; Martín, A.; Menjón, B.; Tomás, M. *Polyhedron* **1996**, *15*, 3599.

(19) Ara, I.; Falvello, L. R.; Forniés, J.; Lalinde, E.; Martín, A.; Martínez, F.; Moreno, M. T. *Organometallics* **1997**, *16*, 5392.

symmetrically flank the central singlet due to P3 and P4, from which $^3J_{P3-P4}$, $^1J_{Pt6-P3}$, and $^2J_{Pt7-P3}$ values can be calculated. From the analysis of these three isotopomers the values of δ_P, J_{Pt-P}, and J_{P-P} can be extracted (see Table 2). Some lines of minor intensity due to the other isotopomers (D−F) are also observed. The spectra simulated using the values of the chemical shifts and coupling constants summarized in Table 2 are in agreement with observation. The resonances of the P atoms of the PPh_2 groups in **4**−**6** (170 ppm region) are shifted to lower fields than those of the starting materials (−100 ppm region). It is well documented that a deshielding of the ^{31}P resonances (usually in the range from +50 to +400 ppm) in phosphido-bridged complexes may indicate the presence of metal−metal bonds supported by the phosphido ligand. A relationship between the angular parameters at the phosphorus atom and the corresponding $\delta^{31}P$ has been observed previously, the closing of the M−P−M′ angle leading to deshielding at the P atom. We have previously observed that δP values can render important information about M−P−M angles in singly bridged diphenylphosphido or dibridged bis(diphenylphosphido) complexes, although single and double bridges cannot be compared to each other in this context.[4b] The Pt(1)−P(1)−Pt(2) and Pt(1)−P(2)−Pt(3) angles in cluster **4** are rather acute (77.64(8)° and 76.49(7)°, respectively), the Pt(1)−Pt(2) and Pt(1)−Pt(3) distances are short (2.791(1) and 2.791(1) Å, respectively), and the δP is 172.8 ppm. Analogous Pt−P−M angles and chemical shifts have been found for other singly bridged diphenylphosphido ligands which support metal−metal bonds (78.28(9)°, δP = 179.5 ppm for $[NBu_4][Pt_3(\mu\text{-}PPh_2)_2(C_6F_5)_5]$;[3b] 75.99(5)°, δP = 180.3 ppm for $[Pt_4(\mu\text{-}PPh_2)_4(C_6F_5)_4]$;[4c] 78.60(7)°, δP = 152.7 ppm for $[Pd_2Pt_2(\mu\text{-}PPh_2)_3(C_6F_5)_3(PPh_2C_6F_5)(CO)]$[4b]). Nevertheless, for similar Pt−P−M angles in dibridged bis(diphenyphosphido) complexes with metal−metal bonds lower field values of the chemical shifts have been observed (73.47(5)°, δP = 281.7 ppm for $[Pt_2(\mu\text{-}PPh_2)_2(C_6F_5)_4]$;[2c] 72.90(7)° and 71.91(7)°, δP = 257.2 and 275.7 ppm for $[Pt_4(\mu\text{-}PPh_2)_4(C_6F_5)_4(CO)_2]$;[4b] 70.57(6)°, δP = 226.8 ppm for $[PdPt(\mu\text{-}PPh_2)_2(C_6F_5)_2(PPh_3)]$[2b]). These results confirm our earlier observation of a relationship[4c] between the δP values and the presence of one or two PPh_2 groups acting as bridging ligands between the two metal centers: In our experience, the chemical shifts of the P atoms in singly bridged diphenylphosphido complexes with metal−metal bonds appear at higher field than those of P atoms in dibridged bis(diphenylphosphido) complexes with metal−metal bonds. A correlation between Pt−Pμ bond lengths and $^1J_{Pt-P\mu}$ values has been found[20] in closely related dinuclear systems (longer Pt−P bonds being associated with a diminution of the coupling constants). In cluster **4** the J_{15} value (2356 Hz, average Pt−P distance 2.244 Å) is lower than the J_{16} value (2640 Hz, average Pt−P distance 2.236 Å). The $^1J_{Pt-P\mu}$ values in **4**−**6** are not very different from those observed for $[Pt_3(\mu\text{-}PPh_2)_3Ph(PPh_3)_2]$,[10] $[Pt_3(\mu\text{-}PBu^t_2)_3H(CO)_2]$,[9] and $[Pt_3(\mu\text{-}PPh_2)_2(\mu\text{-}H)(PPh_3)_3]^+$,[12] although it has been found that the $^1J_{Pt-P\mu}$ values are very sensitive to changes in the ligands on the Pt center. The value of the coupling constants between the two P atoms of the PPh_2 groups, $^2J_{P-P}$, are large (313 Hz in **4**), probably due to the pseudo *trans* disposition of the two groups (P−Pt−P angle in **4** 161.26°). For a series of phosphido-bridged dinuclear compounds it has been reported that the P−M−P angle is extremely important in determining the magnitude of $^2J_{P-P}$.[21] Thus the $^2J_{P-P}$ value in **4** is somewhat larger than that found in the 42-electron cluster $[Pt_3(\mu\text{-}PPh_2)_2(\mu\text{-}H)(PPh_3)_3]^+$, 260 Hz, which shows a smaller P−Pt−P angle, 156.1(1)°. Nevertheless in the 44-electron cluster $[Pt_3(\mu\text{-}PBu^t_2)_3H(CO)_2]$ this coupling constant is smaller, 164 Hz, whereas the P−Pt−P angle is larger, 169.6(1)°. All these data demonstrate again that it is necessary to be very cautious when extracting structural information from J_{Pt-P} and J_{P-P} values in phosphido complexes.

The ^{19}F NMR spectra of **4**−**6** in $CDCl_3$ solution (see Experimental Section) show the same pattern and indicate that in all cases there is a bridging C_6F_5 group.[16,18] Each spectrum shows six signals (intensity ratio 2:2:1:2:1:2) due to the two inequivalent C_6F_5 ligands. Three of the signals correspond to the terminal C_6F_5 group and the other three to the bridging one. Within each group (bridging and terminal) the two *ortho* fluorine atoms are equivalent, as are the two *meta* fluorines. As in previous cases, the signals due to the *o*-F and *p*-F atoms of the bridging C_6F_5 ring appear in an unaccustomed region (ca. −95 and −150 ppm, respectively) with respect to these signals for the terminal C_6F_5 group (ca. −115 and −165 ppm, respectively). The signals due to the *o*-F atoms of both types of C_6F_5 ligand show platinum satellites, and the intensity ratio of the signal at ca. −95 ppm (*o*-F atoms of μ-C_6F_5) is 1:8:17:8:1, as is to be expected due to the equivalence of the two platinum atoms bonded to this C_6F_5 group. The $^3J_{Pt-F}$ value for this bridging pentafluorophenyl ligand is smaller than the values usually observed for terminal pentafluorophenyl groups. All these data are in agreement with the solid-state structure established for cluster **4**.

The IR spectra of complexes **4**−**6** show only one absorption in the 800 cm^{-1} region (two absorptions of similar intensity were observed for complexes **1**−**3**).

Complexes **4**−**6** are new examples of phosphido platinum complexes with mixed oxidation states (II, I, I) and with a total valence electron count of 42. As far as we know, only two phosphido clusters of this type have been fully (X-ray) characterized, $[Pt_3(\mu\text{-}PPh_2)_2(\mu\text{-}H)(PPh_3)_3]^+$ [12a] and $[Pt_3(\mu\text{-}Ph)(\mu\text{-}PPh_2)(\mu\text{-}SO_2)Ph(PPh_3)_2]$.[13] The reaction process that renders **4**−**6** is remarkable since it seems to be a general process. Although the condensation of an M(II) dinuclear derivative with a mononuclear M(0) compound to afford an $M^I_2M^{II}$ triangulo cluster has been reported as a potentially general method, this synthetic procedure has not actually been used with generality. Thus, although the synthesis of $[Pd_3(\mu\text{-}PPh_2)_3(PPh_3)_3]^+$ [22] from $[Pd(PPh_3)_4]$ and $[Pd_2(\mu\text{-}PPh_2)_2Cl_2(PPh_2H)_2]$ has been reported, the yield of triangulo Pd_3 is very low (ca. 15%) and the prolonged heating of $[PdCl(PPh_3)_3][BF_4]$ in tetrahydrofuran provides a better entry into the chemistry of these palladium systems. Nevertheless, $[PtCl(PPh_3)_3][BF_4]$ remains unchanged by heating in tetrahydrofuran. The

(20) (a) Powell, J.; Sawyer, J. F.; Stainer, M. V. R. *Inorg. Chem.* **1989**, *28*, 4461. (b) Powell, J.; Fuchs, E.; Gregg, M. R.; Phillips, J.; Stainer, M. V. R. *Organometallics* **1990**, *9*, 387.

(21) Brandon, J. B.; Dixon, K. R. *Can. J. Chem.* **1981**, *59*, 1188.

synthesis of the 44-electron cluster $[Pt_3(\mu\text{-}PPh_2)_3Ph(PPh_3)_2]$ has been carried out[8,10,23] by the complicated pyrolysis of zerovalent platinum complexes such as $[Pt(PPh_3)_4]$ or $[Pt(PPh_3)_2(C_2H_4)]$. These reactions proceed by cleavage of P−C bonds and formation of μ-PPh_2 and Pt-phenyl linkages. The formation of $[Pt_3(\mu\text{-}PBu^t_2)_3H(CO)_2]$ from $[Pt_2(\mu\text{-}PBu^t_2)_2(H)_2(PBu^t_2H)_2]$ and CO (or $[Pt(PPh_3)_2(CO)_2]$) has been elegantly explained by Leoni et al.[9] The process is carried out at high temperature (100 °C) and it starts by CO-induced intramolecular P−H reductive elimination. The synthesis of the 42-electron triangulo triplatinum cluster $[Pt_3(\mu\text{-}PPh_2)(\mu\text{-}Ph)(\mu\text{-}SO_2)(PPh_3)_2]$[13] has been carried out by refluxing a suspension of $[Pt(1,2\ \eta\text{-}C_4H_5R)(SO_2)(PPh_3)_2\cdot 2SO_2]$ in benzene, whereas $[Pt_3(\mu\text{-}PPh_2)_2(\mu\text{-}H)(PPh_3)_3][BF_4]$[12a] has been synthesized by UV irradiation of an ethanolic solution of $[Pt(C_2O_4)(PPh_3)_2]$. As can be seen, all the ligands present in complexes **4**−**6** were already present in the starting materials, and the syntheses of these trinuclear complexes from **1**−**3** involve only the migration of C_6F_5, PPh_2R, and PPh_2 groups but not the formation of new ligands.

The reaction processes that render **4**−**6** take place under very mild conditions (room temperature) and contrast with the drastic conditions that have to be used for the formation of the triangular cores in other Pt_3 clusters. Since it has been demonstrated that C_6F_5[16] and PPh_3[19,24] can bridge two metal centers and that there are some complexes in which one PPh_2 group acts as a bridging ligand between three metal centers,[3b,4b,c] the migration of the ligands between the metal centers could be facilitated through the formation of permanent (μ^2-C_6F_5) or transitory (μ^2-PR_3, μ^3-PR_2) bridging interactions.

Reaction of $[Pt_3(\mu\text{-}PPh_2)_2(\mu\text{-}C_6F_5)(C_6F_5)(PPh_3)_2]$, 4, with Lewis Acids. This trinuclear 42 valence electron count complex behaves as a Lewis base. The reactions of **4** with Ag(I) Lewis acid complexes result in the corresponding neutralization processes. So, the addition of $AgClO_4$ to CH_2Cl_2 solutions of complex **4** in 1:1 molar ratio gives the neutral heterotetranuclear cluster $[Pt_3Ag(\mu\text{-}PPh_2)_2(\mu\text{-}C_6F_5)(C_6F_5)(OClO_3)(PPh_3)_2]$, **7** (Scheme 2, c). The cationic cluster $[Pt_3Ag(\mu\text{-}PPh_2)_2(\mu\text{-}C_6F_5)(C_6F_5)(PPh_3)_3][ClO_4]$, **8**, is obtained (Scheme 2, d) by using $[Ag(OClO_3)(PPh_3)]$ as Lewis acid. No reactions between triangulo-Pt_3 phosphido complexes with 42 valence electron counts and Lewis acid complexes have been described to date, although the reaction of the more electron-rich (44VEC) $[Pt_3(\mu\text{-}PPh_2)_3Ph(PPh_3)_3]$ with silver triflate forms the corresponding adduct.[25] Complexes **7** and **8** were characterized by elemental analysis and IR and NMR spectroscopy. A single-crystal X-ray diffraction study has been carried out for complex **7**.

Crystal Structure of $[Pt_3Ag(\mu\text{-}PPh_2)_2(\mu\text{-}C_6F_5)(C_6F_5)(OClO_3)(PPh_3)_2]$. The structure of complex **7** together with the atom-labeling scheme is shown in

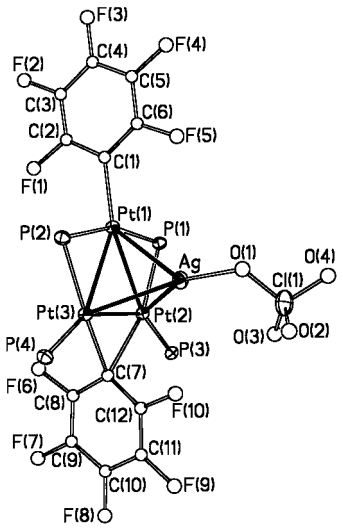

Figure 3. Structure of $[Pt_3Ag(\mu\text{-}PPh_2)_2(\mu\text{-}C_6F_5)(C_6F_5)(OClO_3)(PPh_3)_2]$ (**7**). Phenyl rings have been omitted for the sake of clarity.

Table 3. Selected Bond Lengths (Å) and Angles (deg) for $[Pt_3Ag(\mu\text{-}PPh_2)_2(\mu\text{-}C_6F_5)(C_6F_5)(OClO_3)(PPh_3)_2]\cdot 2CH_2Cl_2$ (7·2CH_2Cl_2)

Pt(1)−Pt(2)	2.838(1)	Pt(1)−Pt(3)	2.835(1)	Pt(2)−Pt(3)	2.794(1)
Pt(1)−Ag	2.778(1)	Pt(2)−Ag	2.813(1)	Pt(3)−Ag	2.795(1)
Pt(1)−C(1)	2.046(6)	Pt(1)−P(1)	2.251(2)	Pt(1)−P(2)	2.264(2)
Pt(2)−P(1)	2.227(2)	Pt(2)−P(3)	2.270(2)	Pt(2)−C(7)	2.349(6)
Pt(3)−C(7)	2.172(6)	Pt(3)−P(2)	2.259(2)	Pt(3)−P(4)	2.268(2)
Ag−O(1)	2.236(6)				

C(1)−Pt(1)−P(1)	99.60(17)	C(1)−Pt(1)−P(2)	99.96(18)
P(1)−Pt(1)−P(2)	160.33(6)	Ag−Pt(1)−Pt(3)	59.723(14)
Ag−Pt(1)−Pt(2)	60.103(17)	Pt(3)−Pt(1)−Pt(2)	59.006(10)
P(1)−Pt(2)−P(3)	101.48(6)	P(1)−Pt(2)−C(7)	160.24(16)
P(3)−Pt(2)−C(7)	97.83(16)	Pt(3)−Pt(2)−Ag	59.808(16)
Pt(3)−Pt(2)−Pt(1)	60.450(9)	Ag−Pt(2)−Pt(1)	58.886(16)
C(7)−Pt(3)−P(2)	164.36(16)	C(7)−Pt(3)−P(4)	95.60(16)
P(2)−Pt(3)−P(4)	98.34(6)	Pt(2)−Pt(3)−Ag	60.429(17)
Pt(2)−Pt(3)−Pt(1)	60.544(10)	Ag−Pt(3)−Pt(1)	59.113(14)
O(1)−Ag−Pt(1)	138.77(17)	O(1)−Ag−Pt(3)	139.2(2)
Pt(1)−Ag−Pt(3)	61.164(13)	O(1)−Ag−Pt(2)	153.78(18)
Pt(1)−Ag−Pt(2)	61.012(13)	Pt(3)−Ag−Pt(2)	59.764(13)
Pt(2)−P(1)−Pt(1)	78.66(5)	Pt(3)−P(2)−Pt(1)	77.64(5)

Figure 3. For the sake of clarity, the phenyl rings of the PPh_2 groups have been omitted from the figure. Selected bond distances and angles are listed in Table 3. The structure is very similar to that described for complex **4** with the addition of an "$AgOClO_3$" fragment. Again, the three platinum atoms form a nearly equilateral triangle, with the Pt−Pt distances (Pt(1)−Pt(2) 2.838(1) Å, Pt(1)−Pt(3) 2.835(1) Å, Pt(2)−Pt(3) 2.794(1) Å) slightly longer than in **4**, and in agreement with the presence of Pt−Pt bonds. The silver atom caps the Pt_3 triangle at 2.29 Å away from the best plane defined by all of the Pt and P atoms and just above the center of the Pt_3 triangle. The three Pt−Ag bond distances (Pt(1)−Ag 2.778(1) Å, Pt(2)−Ag 2.813(1) Å, and Pt(1)−Ag 2.795(1) Å) are very similar. In fact, the four metal atoms define the corners of an almost perfect tetrahedron. The coordination environment of the silver atom is completed by an oxygen of a covalently bonded perchlorate group.

As mentioned above, the structural parameters found in the "Pt_3" fragment are very similar to the ones found in **4**. In **7**, the terminal pentafluorophenyl ligand is slightly more displaced from the basal plane, in the opposite direction from the silver atom (C(1) 0.31 Å, C(4)

(22) Cartwright, S. J.; Dixon, K. R.; Rattray, A. D. *Inorg. Chem.* **1980**, *19*, 1120.
(23) (a) Bennet, M. A.; Berry, D. E.; Dirnberger, T.; Hockless, D. C. R.; Wenger, E. *J. Chem. Soc., Dalton Trans.* **1998**, 2367. (b) Bender, R.; Bouaoud, S.-E.; Braunstein, P.; Dusausoy, Y.; Merabet, N.; Raya, J.; Rouag, D. *J. Chem. Soc., Dalton Trans.* **1999**, 735.
(24) Kannan, S.; James, A. J.; Sharp, P. R. *J. Am. Chem. Soc.* **1998**, *120*, 215.
(25) Archambault, C.; Bender, R.; Braunstein, P.; De Cian, A.; Fischer, J. *J. Chem. Soc., Chem. Commun.* **1996**, 2729.

0.76 Å, F(3) 0.96 Å), probably in order to avoid steric repulsions. At the same time, the bridging C_6F_5 group is closer to the Pt_3 plane than in **4** (C(7) 0.12 Å, C(10) 0.47 Å, F(8) 0.64 Å). The dihedral angles between the best plane defined by the Pt and P atoms and the C_6F_5 rings are 84.2° and 89.9° for the terminal and bridging groups, respectively. The rest of the parameters involving the Pt_3P_4 core are not significantly different from **4**.

As in complex **4**, the bridging pentafluorophenyl group displays perceptibly different Pt−C_{ipso} distances (Pt(2)−C(7) 2.349(6) Å and Pt(3)−C(7) 2.172(6) Å), indicating an asymmetric bonding.

The $^{31}P\{^1H\}$ NMR spectra of **7** and **8** in $CDCl_3$ show a pattern similar to those of **4**−**6**, and the spectral analysis of each has been carried out, as for clusters **4**−**6**. All data that can be calculated from the spectra are collected in Table 2. The signal due to the P atoms of the two PPh_2 groups appears in the 160 ppm region, the central signal being a sharp singlet. The signal due to the P atoms of the two equivalent triphenylphosphines bonded to the platinum centers appears in the 30 ppm region as a doublet ($^2J_{Ag-P} \approx 31$ Hz, **7**, and 29 Hz, **8**), because of the poorly resolved couplings with ^{109}Ag (48.2%) and ^{107}Ag (51.8%) atoms. In complex **8** the signal due to the P atom of the "$AgPPh_3$" fragment appears at 13.9 ppm as a doublet (ca. 610 Hz) of very complex multiplets due to coupling with ^{109,107}Ag and ^{195}Pt atoms. The two $^1J_{Ag-P}$ and the two $^2J_{Pt-P}$ values cannot be extracted from these multiplets.

The ^{19}F NMR spectra of **7** and **8** at room temperature show eight signals of intensity ratio 1:1:2:1:1:1:1:2 (see Experimental Section). In the *o*-F region one signal for the two *o*-F atoms of the terminal C_6F_5 group and two signals (at lower field) for the two *o*-F atoms of the μ-C_6F_5 ring are observed. The two *m*-F atoms of the bridging μ-C_6F_5 ring appear as two signals at lower field than the signal due to the two *m*-F atoms of the terminal C_6F_5 group. Finally, one signal is observed for each *p*-F atom of each C_6F_5 ligand. These spectra show the inequivalence in solution of the two *o*-F atoms as well as the two *m*-F atoms of the bridging pentafluorophenyl ligand, in agreement with the solid-state structure of cluster **7**. Nevertheless, the two *o*-F atoms as well as the *m*-F atoms of the terminal C_6F_5 ligand are equivalent in solution, indicating that at room temperature the rotation of the Pt−C_{ipso} is not inhibited. When the spectra are recorded at low temperature, the two *o*-F atoms of the terminal C_6F_5 group are inequivalent while the *m*-F atoms are isochronous. Variable-temperature ^{19}F NMR spectra for **7** in CD_2Cl_2 reveal the coalescence of the two *o*-F signals of the terminal C_6F_5 at 203 K. The approximation to Eyring's equation leads to a $\Delta G^{\ddagger}$ value of 37 kJ mol^{-1} at the coalescence temperature for Pt−C_{ipso} bond rotation.

In all cases the *o*-F−^{195}Pt couplings involving the bridging C_6F_5 groups are small, since only broadening of the signals can be observed. Moreover the two signals due to the *o*-F atoms of the terminal C_6F_5 group in **7** are broad even at 188 K and $^3J_{Pt-F}$ cannot be calculated.

The ^{19}F NMR spectrum of **7** in acetone at room temperature is similar to that obtained in $CDCl_3$, indicating that the donor−acceptor Pt−Ag bonds are also present in the donor solvent; that is, the Pt−Ag bonds are not displaced by the donor solvent as occurs in other complexes containing this type of donor−acceptor bond.[26]

Aiming to obtain clusters of higher nuclearity, we have carried out the reaction of **4** with more than 2 equiv of $AgClO_4$, but only complex **7** is obtained (Scheme 2, c′). Moreover, the reaction of cluster **4** with a CH_2Cl_2 solution of **7** in 1:1 molar ratio at room temperature renders only a purple solid which is a mixture of **4** and **7** (NMR identification) and not the heptanuclear cluster (Scheme 2, f). Nevertheless, a CH_2Cl_2 solution of **7** reacts with 1 equiv of PPh_3, yielding (Scheme 2, e) the cationic **8**.

Experimental Section

C and H analyses, IR, NMR, and mass spectra were performed as described elsewhere.[4c] Literature methods were used to prepare the starting materials $[NBu_4]_2[(C_6F_5)_2Pt(\mu\text{-}PPh_2)_2Pt(\mu\text{-}Cl)_2Pt(\mu\text{-}PPh_2)_2Pt(C_6F_5)_2]$,[2a] $[Pt(C_7H_{10})_3]$,[27] and $[Ag(OClO_3)PPh_3]$.[28] All the reactions have been carried out under N_2.

Safety Note: Perchlorate salts of metal complexes with organic ligands are potentially explosive. Only small amounts of material should be prepared, and these should be handled with great caution.

Preparation of $[Pt_2(\mu\text{-}PPh_2)_2(C_6F_5)_2(PPh_2R)_2]$. R = Ph (1). To a solution of $[NBu_4]_2[(C_6F_5)_2Pt(\mu\text{-}PPh_2)_2Pt(\mu\text{-}Cl)_2Pt(\mu\text{-}PPh_2)_2Pt(C_6F_5)_2]$ (0.650 g, 0.237 mmol) in CH_2Cl_2 (15 mL)/MeOH (5 mL) was added PPh_3 (0.256 g, 0.976 mmol). The solution was stirred at room temperature for 15 h, and a yellow suspension was obtained. The mixture was evaporated to ca. 10 mL, and the resulting yellow solid **1** was filtered off, washed with MeOH (3 × 1 mL), and vacuum-dried (0.364 g, 47%). Anal. Found (calcd for $C_{72}F_{10}H_{50}P_4Pt_2$): C, 53.9 (53.4); H, 3.25 (3.1). IR (X-sensitive C_6F_5, cm^{-1}): 783 and 774. FAB-MS: *m*/*z* 1619 ($[M]^+$). ^{19}F NMR (CD_2Cl_2): δ −114.9 (4 *o*-F, J_{PtF} = 320 Hz), −166.1 (4 *m*-F), −166.4 (2 *p*-F) ppm. $^{31}P\{^1H\}$ NMR (CD_2Cl_2): δ 15.7 (PPh_3, $J_{Pt(2)P}$ = 1425 Hz, *N* = 251 Hz), −97.5 (μ-PPh_2, $J_{Pt(1)P} \approx J_{Pt(2)P} \approx$ 1723 Hz) ppm.

Complexes **2** and **3** were prepared as for **1**.

R = Me (2). $[NBu_4]_2[(C_6F_5)_2Pt(\mu\text{-}PPh_2)_2Pt(\mu\text{-}Cl)_2Pt(\mu\text{-}PPh_2)_2Pt(C_6F_5)_2]$ (0.500 g, 0.182 mmol) and PPh_2Me (0.27 mL, 1.4 mmol) were used to prepare **2**, which was obtained as a yellow solid (0.290 g, 53%). Anal. Found (calcd for $C_{62}F_{10}H_{46}P_4Pt_2$): C, 49.7 (49.8); H, 3.5 (3.1). IR (X-sensitive C_6F_5, cm^{-1}): 782 and 772. FAB-MS: *m*/*z* 1495 ($[M]^+$). ^{19}F NMR (CD_2Cl_2): δ −115.2 (4 *o*-F, J_{PtF} = 311 Hz), −166.2 (6 *m*- + *p*-F) ppm. $^{31}P\{^1H\}$ NMR (CD_2Cl_2): δ 0.9 (PPh_2Me, $J_{Pt(2)P}$ = 2145 Hz, *N* = 253 Hz), −104.3 (μ-PPh_2, $J_{Pt(1)P} \approx J_{Pt(2)P} \approx$ 1689 Hz) ppm.

R = Et (3). $[NBu_4]_2[(C_6F_5)_2Pt(\mu\text{-}PPh_2)_2Pt(\mu\text{-}Cl)_2Pt(\mu\text{-}PPh_2)_2Pt(C_6F_5)_2]$ (0.442 g, 0.161 mmol) and PPh_2Et (0.27 mL, 1.3 mmol) were used to prepare **3**, which was obtained as a yellow solid (0.315 g, 64%). Anal. Found (calcd for $C_{64}F_{10}H_{50}P_4Pt_2$): C, 50.5 (50.5); H, 3.1 (3.3). IR (X-sensitive C_6F_5, cm^{-1}): 783 and 773. FAB-MS: *m*/*z* 1523 ($[M]^+$). ^{19}F NMR (CD_2Cl_2): δ −115.0 (4 *o*-F, J_{PtF} = 321 Hz), −166.3 (6 *m*- + *p*-F) ppm. $^{31}P\{^1H\}$ NMR (CD_2Cl_2): δ 10.6 (PPh_2Et, $J_{Pt(2)P}$ = 2138 Hz, *N* = 254 Hz), −109.3 (μ-PPh_2, $J_{Pt(1)P} \approx J_{Pt(2)P} \approx$ 1717 Hz) ppm.

Preparation of $[Pt_3(\mu\text{-}PPh_2)_2(\mu\text{-}C_6F_5)(C_6F_5)(PPh_2R)_2]$. R = Ph (4). To a suspension of **1** (0.547 g, 0.338 mmol) in toluene (20 mL) was added $[Pt(C_7H_{10})_3]$ (0.164 g, 0.343 mmol). The mixture was stirred at room temperature for 22 h. The very dark purple solution was evaporated to ca. 1 mL, and

(26) (a) Usón, R.; Forniés, J.; Menjón, B.; Cotton, F. A.; Falvello, L. R.; Tomás, M. *Inorg. Chem.* **1985**, *24*, 4651. (b) Usón, R.; Forniés, J.; Tomás, M.; Ara, I. *J. Chem. Soc., Dalton Trans.* **1990**, 3151.
(27) Crascall, L. E.; Spencer, J. L. *Inorg. Synth.* **1990**, *28*, 126.
(28) Cotton, F. A.; Falvello, L. R.; Usón, R.; Forniés, J.; Tomás, M.; Casas, J. M.; Ara, I. *Inorg. Chem.* **1987**, *26*, 1366.

Table 4. Crystal Data and Structure Refinement for $[Pt_3(\mu\text{-}PPh_2)_2(\mu\text{-}C_6F_5)(C_6F_5)(PPh_3)_2]$ (4) and $[Pt_3Ag(\mu\text{-}PPh_2)_2(\mu\text{-}C_6F_5)(C_6F_5)(OClO_3)(PPh_3)_2]\cdot 2CH_2Cl_2$ (7·2CH_2Cl_2)

	4	**7**·2CH_2Cl_2
empirical formula	$C_{72}H_{50}F_{10}P_4Pt_3$	$C_{72}H_{50}AgClF_{10}O_4P_4Pt_3\cdot 2CH_2Cl_2$
unit cell dimens, *a* (Å)	12.822(2)	11.4288(7)
b (Å)	15.606(2)	14.1307(6)
c (Å)	16.845(2)	22.4596(12)
α (deg)	102.77(2)	93.525(7)
β (deg)	98.72(2)	90.552(16)
γ (deg)	105.16(2)	94.159(10)
volume (Å^3), *Z*	3093.3(8), 2	3610.4(3), 2
wavelength (Å)	0.71073	
temperature (K)	293(1)	150(1)
radiation	graphite-monochromated Mo Kα	
space group	$P\bar{1}$	$P\bar{1}$
cryst dimens (mm)	0.55 × 0.10 × 0.06	0.48 × 0.31 × 0.17[a] 0.38 × 0.24 × 0.16[b]
abs coeff (mm^{-1})	6.945	6.410
transmn factors	1.000, 0.621	1.000, 0.501[a] 0.924, 0.473[b]
abs corr	*ψ* scans	*ψ* scans
diffractometer	Enraf Nonius CAD4	Enraf Nonius CAD4
2*θ* range for data collection (deg)	4.3−50.0 (+*h*, ±*k*, ±*l*)	4.0−50.0 (+*h*, ±*k*, +*l*)
no. of reflns collected	11 383	13 479 (8852[a] + 4627[b])
no. of ind reflns	10854 [*R*(int) = 0.0275]	8158 [*R*(int) = 0.0200][a] 4620 [*R*(int) = 0.0121][b]
goodness-of-fit on F^2	1.014	1.031
final *R* indices [$I > 2\sigma(I)$]	R1 = 0.0403 wR2 = 0.0766	R1 = 0.0340, wR2 = 0.0898
R indices (all data)	R1 = 0.0765 wR2 = 0.0901	R1 = 0.0485 wR2 = 0.0964

[a] Crystal 1 (see Experimental Section). [b]Crystal 2 (see Experimental Section). $wR2 = [\sum w(F_o^2 - F_c^2)^2/\sum wF_o^4]^{0.5}$; $R1 = \sum||F_o| - |F_c||/\sum|F_o|$. Goodness-of-fit = $[\sum w(F_o^2 - F_c^2)^2/N_{obs} - N_{param}]^{0.5}$.

hexane (8 mL) was added. The dark purple solid **4** was filtered off, washed with hexane (3 × 2 mL), and vacuum-dried (0.364 g, 59%). Anal. Found (calcd for $C_{72}F_{10}H_{50}P_4Pt_3$): C, 47.3 (47.7); H, 2.8 (2.8). IR (X-sensitive C_6F_5, cm^{-1}): 781. FAB-MS: *m*/*z* 1814 ([M]$^+$). ^{19}F NMR ($CDCl_3$): *δ* −94.9 (2 *o*-F, *μ*-C_6F_5, J_{PtF} = 157 Hz), −117.0 (2 *o*-F, J_{PtF} = 393 Hz), −148.7 (1 *p*-F, *μ*-C_6F_5), −161.4 (2 *m*-F, *μ*-C_6F_5), −165.4 (1 *p*-F), −166.6 (2 *m*-F) ppm.

R = Me (5). Complex **5** was prepared similarly by reacting **2** (0.111 g, 0.074 mmol) and $[Pt(C_7H_{10})_3]$ (0.040 g, 0.083 mmol) at room temperature for 5 days. **5** was formed as a purple solid (0.044 g, 35%). Anal. Found (calcd for $C_{62}F_{10}H_{46}P_4Pt_3$): C, 43.9 (44.1); H, 2.8 (2.7). IR (X-sensitive C_6F_5, cm^{-1}): 780. FAB-MS: *m*/*z* 1690 ([M]$^+$). ^{19}F NMR ($CDCl_3$): *δ* −96.5 (2 *o*-F, *μ*-C_6F_5, J_{PtF} = 177 Hz), −116.8 (2 *o*-F, J_{PtF} = 399 Hz), −147.3 (1 *p*-F, *μ*-C_6F_5), −161.4 (2 *m*-F, *μ*-C_6F_5), −165.2 (1 *p*-F), −166.4 (2 *m*-F) ppm.

R = Et (6). Complex **6** was prepared in the same way from **3** (0.182 g, 0.119 mmol) and $[Pt(C_7H_{10})_3]$ (0.061 g, 0.13 mmol). **6** was obtained as a purple solid (0.091 g, 44%). Anal. Found (calcd for $C_{64}F_{10}H_{50}P_4Pt_3$): C, 44.9 (44.7); H, 2.95 (2.9). IR (X-sensitive C_6F_5, cm^{-1}): 779. FAB-MS: *m*/*z* 1718 ([M]$^+$). ^{19}F NMR ($CDCl_3$): *δ* −94.6 (2 *o*-F, *μ*-C_6F_5, J_{PtF} = 166 Hz), −117.0 (2 *o*-F, J_{PtF} = 392 Hz), −150.0 (1 *p*-F, *μ*-C_6F_5), −162.1 (2 *m*-F, *μ*-C_6F_5), −165.3 (1 *p*-F), −166.6 (2 *m*-F) ppm.

Preparation of $[Pt_3Ag(\mu\text{-}PPh_2)_2(\mu\text{-}C_6F_5)(C_6F_5)(OClO_3)(PPh_3)_2]$ (7). To a solution of **4** (0.100 g, 0.055 mmol) in CH_2Cl_2 (20 mL) was added $AgClO_4$ (0.020 g, 0.096 mmol), and the mixture was stirred, at room temperature and in the dark, for 15 h. The mixture was filtered through Celite and the filtrate evaporated to ca. 2 mL, whereupon a purple solid began to crystallize. Hexane (5 mL) was added, and the resulting solid **7** was filtered off, washed with hexane (2 × 2 mL), and vacuum-dried (0.085 g, 76%). Anal. Found (calcd for $AgC_{72}ClF_{10}H_{50}O_4P_4Pt_3$): C, 42.5 (42.8); H, 2.5 (2.5). IR (X-sensitive C_6F_5, cm^{-1}): 785. FAB-MS: *m*/*z* 1922 ([M − ClO_4]$^+$). ^{19}F NMR ($CDCl_3$, 295 K): *δ* −82.8 (1 *o*-F, *μ*-C_6F_5), −96.7 (1 *o*-F, *μ*-C_6F_5), −117.6 (2 *o*-F, J_{PtF} = 401.0 Hz), −142.8 (1 *p*-F, *μ*-C_6F_5), −157.1 (1 *m*-F, *μ*-C_6F_5), −159.2 (1 *m*-F, *μ*-C_6F_5), −162.7 (1 *p*-F), −165.2 (2 *m*-F) ppm. ^{19}F NMR (CD_2Cl_2, 188 K): *δ* −82.4 (1 *o*-F, *μ*-C_6F_5), −95.1 (1 *o*-F, *μ*-C_6F_5), −115.4 (1 *o*-F), −117.4 (1 *o*-F), −142.5 (1 *p*-F, *μ*-C_6F_5), −152.3 (1 *m*-F, *μ*-C_6F_5), −162.0 (1 *m*-F, *μ*-C_6F_5), −162.7 (1 *p*-F), −164.5 (2 *m*-F) ppm.

Preparation of $[Pt_3Ag(\mu\text{-}PPh_2)_2(\mu\text{-}C_6F_5)(C_6F_5)(PPh_3)_3][ClO_4]$ (8). (a) To a solution of **4** (0.100 g, 0.055 mmol) in 20 mL of CH_2Cl_2 was added $[Ag(OClO_3)PPh_3]$ (0.026 g, 0.055 mmol), and the mixture was stirred, at room temperature and in the dark, for 1 h. The solution was evaporated to ca. 1 mL, hexane (2 mL) was added, and the resulting purple solid **8** was filtered off, washed with *n*-hexane (2 × 2 mL), and dried under vacuum. Yield: 0.103 g, 82%. (b) To a solution of **7** (0.053 g, 0.026 mmol) in CH_2Cl_2 (20 mL) was added PPh_3 (0.007 g, 0.03 mmol). After 45 min stirring, the solution was evaporated to ca. 1 mL, hexane was added (2 mL), and the resulting solid **8** was filtered off, washed with hexane (2 × 2 mL), and dried under vacuum (0.040 g, 68%). Anal. Found (calcd for $AgC_{90}ClF_{10}H_{65}O_4P_5Pt_3$): C, 47.2 (47.3); H, 2.95 (2.9). IR (X-sensitive C_6F_5, cm^{-1}): 785. FAB-MS: *m*/*z* 2184 ([M − ClO_4]$^+$). ^{19}F NMR ($CDCl_3$, 295 K): *δ* −83.6 (1 *o*-F, *μ*-C_6F_5), −90.9 (1 *o*-F, *μ*-C_6F_5), −116.9 (2 *o*-F, J_{PtF} = 371 Hz), −142.8 (1 *p*-F, *μ*-C_6F_5), −151.1 (1 *m*-F, *μ*-C_6F_5), −160.8 (1 *m*-F, *μ*-C_6F_5), −161.3 (1 *p*-F), −164.5 (2 *m*-F) ppm. ^{19}F NMR ($CDCl_3$, 218 K): *δ* −83.8 (1 *o*-F, *μ*-C_6F_5), −90.1 (1 *o*-F, *μ*-C_6F_5), −115.5 (1 *o*-F, J_{PtF} = 397 Hz), −117.6 (1 *o*-F, J_{PtF} = 352 Hz), −143.5 (1 *p*-F, *μ*-C_6F_5), −150.3 (1 *m*-F, *μ*-C_6F_5), −161.6 (1 *m*-F, *μ*-C_6F_5), −161.9 (1 *p*-F), −164.2 (2 *m*-F) ppm.

Crystal Structure Analysis of $[Pt_3(\mu\text{-}PPh_2)_2(\mu\text{-}C_6F_5)(C_6F_5)(PPh_3)_2]$ (4) and $[Pt_3Ag(\mu\text{-}PPh_2)_2(\mu\text{-}C_6F_5)(C_6F_5)(OClO_3)(PPh_3)_2]\cdot 2CH_2Cl_2$ (7·2CH_2Cl_2). Crystal data and other details of the structure analysis are presented in Table 4. Suitable crystals of **4** and **7** were obtained by slow diffusion of *n*-hexane into a solution of 0.025 g of $[Pt_3(\mu\text{-}PPh_2)_2(\mu\text{-}C_6F_5)(C_6F_5)(PPh_3)_2]$ or $[Pt_3Ag(\mu\text{-}PPh_2)_2(\mu\text{-}C_6F_5)(C_6F_5)(OClO_3)(PPh_3)_2]$ in CH_2Cl_2 (3 mL) and were mounted at the end of glass fibers. For **4**, unit cell dimensions were determined from 25 centered reflections in the range 20.7° < 2*θ* < 30.1°, each centered at four different goniometer positions. An absorption correction

was applied based on 516 azimuthal scan data. For **7**, due to the instability of the crystals and repeated power failures on the diffractometer and low-temperature device, the crystallographic data set used was obtained by merging the data obtained from two different crystals (see the Supporting Information). Unit cell dimensions were determined from one of the crystals, using 25 reflections in the range $22.6° < 2\theta < 31.7°$, each centered at four different goniometer positions. Absorption corrections were applied independently to the two data sets. For the data from crystal 1, absorption corrections were based on 686 azimuthal scan data, and for crystal 2 the absorption corrections were based on 664 azimuthal scan data.

Both structures were solved by Patterson and Fourier methods. All refinements were carried out using the program SHELXL-93.[29] All non-hydrogen atoms were assigned anisotropic displacement parameters and refined without positional constraints. All hydrogen atoms were constrained to idealized geometries and assigned isotropic displacement parameters of 1.2 times the U_{iso} value of their attached carbon atoms (1.5 times for methyl hydrogen atoms). For **7**·$2CH_2Cl_2$, for the least-squares refinement, the data sets from crystals 1 and 2 were assigned different batch scale factors, which were refined independently, yielding a relative value of 4.122 for crystal 2. The two molecules of dichloromethane present in the structure show some degree of disorder, and of the several models tested, the following led to the best residuals: In one of the molecules, one of the chlorine atoms, Cl(2), shows a disorder over two positions with occupancies 0.7/0.3. In the second molecule, all the atoms (C(74), Cl(4), and Cl(5)) are disordered over two positions with ocupancies 0.6/0.4. For both molecules the C−Cl distances were restrained to accepted values, and for each molecule a common set of anisotropic displacement parameters was used for all of the (non-hydrogen) atoms. Full-matrix least-squares refinement of these models against F^2 converged to final residual indexes given in Table 5. Final difference electron density maps showed no features above 1 e/Å^3 (max./min. 0.95/−0.83 e/Å^3) for **4** and 10 features above 1 e/Å^3 (max./min. 1.65/−1.67 e/Å^3), all of which were either within 1.2 Å of the Pt atoms or in the solvent area for **7**·CH_2Cl_2.

(29) Sheldrick, G. M. *SHELXL-93*, a program for crystal structure determination; University of Göttingen: Germany, 1993.

Acknowledgment. We thank the Dirección General de Enseñanza Superior (Spain) for financial support (Projects PB98-1595-C02-01 and PB98-1593).

Supporting Information Available: Tables of full atomic positional and equivalent isotropic displacement parameters, anisotropic displacement parameters, full bond distances and bond angles, and hydrogen coordinates and anisotropic displacement parameters for the crystal structures of complexes **4** and **7**·$2CH_2Cl_2$. This material is available free of charge via the Internet at http://pubs.acs.org.

OM020036V